A Novel Mixed Integer LP Model to Mitigate the Impact of Light Rail on Conventional Traffic Networks

Paper ID 68

Abstract

As urban traffic congestion is on the increase worldwide, many cities are increasingly looking to inexpensive public transit options such as light rail that operate at street-level and require coordination with conventional traffic networks and signal control. A major concern in light rail installation is whether enough commuters will switch to it to offset the additional constraints it places on traffic signal control and the resulting decrease in conventional vehicle traffic capacity. In this paper, we study this problem and ways to mitigate it through a novel model of optimized traffic signal control subject to light rail schedule constraints solved in a Mixed Integer Linear Programming (MILP) framework. Our key results show that while this MILP approach provides a novel way to optimize fixed-time control schedules subject to light rail constraints, it also enables a novel optimized adaptive signal control method that virtually nullifies the impact of the light rail presence on conventional traffic flow. Ultimately this leads to a win-win situation where both conventional vehicle traffic and light rail commuters benefit through the application of MILP-based optimization to jointly manage public transit and conventional traffic networks.

1 Introduction

As urban traffic congestion is on the increase worldwide with estimated productivity losses in the hundreds of billions of dollars in the U.S. alone and immeasurable environmental impact (Bazzan and Klügl 2013), many cities are increasingly looking to public transit options such as light rail that are less expensive and often more reliable than heavy rail in order to reduce the number of conventional traffic commuters (Thompson 2003). Since light rail often operates at street-level with exclusive right-of-way and requires coordination with conventional traffic networks and signal control, a major concern in light rail installation is whether enough commuters will switch to it to offset the additional constraints it places on traffic signal control.

Unfortunately, many large cities still use some degree of *fixed-time* control (El-Tantawy, Abdulhai, and Abdelgawad 2013) even if they also use *actuated* or *adaptive* control methods such as SCATS (Sims and Dobinson 1980) or SCOOT (Hunt et al. 1981); all of these methods are largely ignorant of light rail schedules, hence posing problems for their effective integration with conventional traffic signal control. A more recent trend in the traffic signal control literature proposes the use of *optimized* controllers (that incorporate elements of both adaptive and actuated control) as evidenced in a variety of approaches including mixed integer linear programming (MILPs) (Lo 1998; Gartner and Stamatiadis 2002; Lin and Wang 2004; He, Head, and Ding 2011; Han, Friesz, and Yao 2012; Anonymous 2016), heuristic search (Lo, Chang, and Chan 1999; He et al. 2010), queuing delay optimization (Varaiya 2013; Li and Zhang 2014), scheduling-driven control (Xie, Smith, and Barlow 2012; Smith et al. 2013), and reinforcement learning (El-Tantawy, Abdulhai, and Abdelgawad 2013). While all of these approaches hold out the promise of more highly optimized traffic control methods, to date, *none* have studied the optimal integration of light rail schedule constraints with their respective methods nor the impact that such integration would have on conventional traffic delay.

To address this deficiency, we leverage a recent MILP model of traffic signal optimization termed the *Queue Transmission Model (QTM)* (Anonymous 2016), where expected traffic queues and flows are continuous variables, traffic signals are discrete variables, and the overall optimization objective is to minimize delay. We extend the QTM model to incorporate light rail schedule constraints and contribute a novel way to optimize fixed-time traffic signal control subject to light rail schedules. As a second major contribution, we also define a novel optimized adaptive signal control variant of the QTM that virtually nullifies the impact of the light rail presence as we show experimentally in both the QTM optimization objective as well as an external microsimulation validation using a fine-grained nonlinear model of traffic flow. Ultimately, these results demonstrate a win-win situation where both conventional vehicle traffic and light rail commuters benefit through the application of MILP-based optimization to jointly manage both light rail schedule priority and conventional traffic networks.

2 The Queue Transmission Model (QTM)

To investigate the impact of light rail schedules on conventional traffic networks we need a model of both traffic flow and light rail constraints. As a model of traffic flow, we leverage the Queue Transmission Model (QTM) (Anonymous

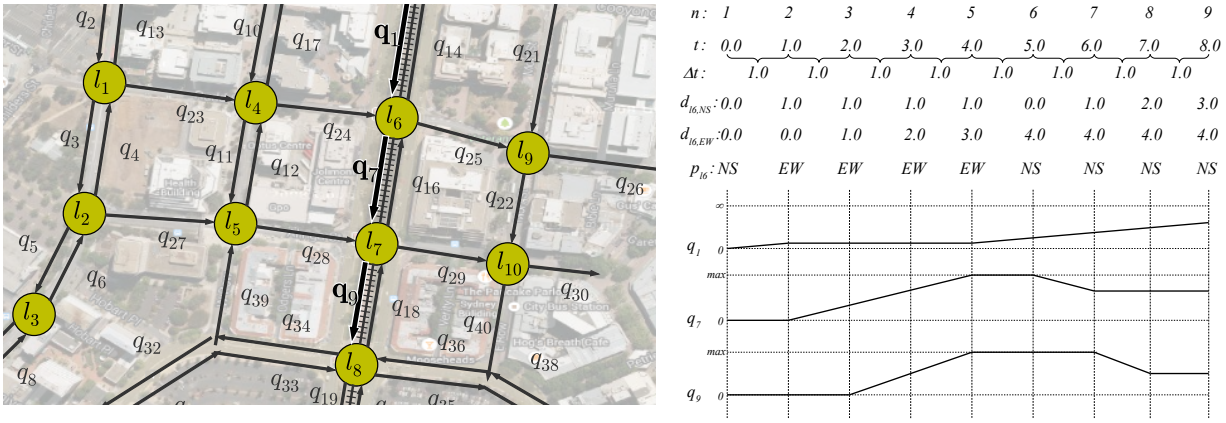

Figure 1: (a) Example of a real traffic network with a central light rail modeled using the QTM. (b) A preview of different QTM model parameters as a function of discretized time intervals indexed by n. For each n, we show the following parameters: the elapsed time t, the time step length Δt, the cumulative duration d of two different light phases for l_6, the phase p of light l_6, and the traffic volume of different queues q linearly interpolated between time points. There is technically a binary p for each phase, but we abuse notation and simply show the current active phase: NS for *north-south green* and EW for *east-west green* assuming the top of the map is north. Here we see that traffic progresses from q_1 to q_7 to q_9 according to light phases and traffic propagation delay. We refer to the QTM model section for precise notation and technical definitions.

2016). Informally, we show an example of a traffic network and the evolution of the variables in a QTM model over time in Figure 1. Formally a QTM is a tuple $(\mathcal{Q}, \mathcal{L}, \vec{\Delta t}, \mathbf{I})$, where $\mathcal{Q}$ and $\mathcal{L}$ are, respectively, the set of queues and lights; $\vec{\Delta t}$ is a vector of size N representing the discretization of the problem horizon $[0, \mathrm{T}]$ and the duration in seconds of the n-th time interval is denoted as Δt_n; and $\mathbf{I}$ is a matrix $|\mathcal{Q}| \times \mathrm{T}$ in which $I_{i,n}$ represents the flow of cars requesting to enter queue i from the outside of the network at time n.

A **traffic light** $\ell \in \mathcal{L}$ is defined as the tuple $(\Psi_\ell^{\min}, \Psi_\ell^{\max}, \mathcal{P}_\ell, \vec{\Phi}_\ell^{\min}, \vec{\Phi}_\ell^{\max})$, where:

- $\mathcal{P}_\ell$ is the set of phases of ℓ;
- $\Psi_\ell^{\min}$ ($\Psi_\ell^{\max}$) is the minimum (maximum) allowed cycle time for ℓ; and
- $\vec{\Phi}_\ell^{\min}$ ($\vec{\Phi}_\ell^{\max}$) is a vector of size $|\mathcal{P}_\ell|$ and $\Phi_{\ell,k}^{\min}$ ($\Phi_{\ell,k}^{\max}$) is the minimum (maximum) allowed time for phase $k \in \mathcal{P}_\ell$.

A **queue** $i \in \mathcal{Q}$ represents a segment of road that vehicles traverse at free flow speed; once traversed, the vehicles are vertically stacked in a stop line queue. Formally, a queue i is defined by the tuple $(\mathrm{Q}_i, \mathrm{T}_i^{\mathrm{p}}, \mathrm{F}_i^{\mathrm{out}}, \vec{F}_i, \vec{Pr}_i, \mathcal{Q}_i^{\mathcal{P}})$ where:

- Q_i is the maximum capacity of i;
- $\mathrm{T}_i^{\mathrm{p}}$ is the time required to traverse i and reach the stop line;
- $\mathrm{F}_i^{\mathrm{out}}$ represents the maximum traffic flow from i to the outside of the modeled network;
- $\vec{F}_i$ and $\vec{Pr}_i$ are vectors of size $|\mathcal{Q}|$ and their j-th entry (i.e., $\mathrm{F}_{i,j}$ and $\mathrm{Pr}_{i,j}$) represent the maximum flow from queue i to j and the turn probability from i to j ($\sum_{j \in \mathcal{Q}} \mathrm{Pr}_{i,j} = 1$), respectively; and
- $\mathcal{Q}_i^{\mathcal{P}}$ denotes the set of traffic light phases controlling the outflow of queue i.

For this work, we assume that $\mathrm{T}_i^{\mathrm{p}}$ is divisible by every different value of Δt_n. This allow us to have queues with different travel time at free flow speed resulting in a non-first order Markovian model as explained in next section.

2.1 Computing Traffic Flows with QTM

In this section, we present how to compute traffic flows using QTM. We assume for the remainder of this section that a *valid* control plan for all traffic lights is fixed and given as parameter; formally, for all $\ell \in \mathcal{L}$, $k \in \mathcal{P}_\ell$, and interval $n \in \{1, \ldots, N\}$, the binary variable $p_{\ell,k,n}$ is known a priori and indicates if phase k of light ℓ is active (i.e., $p_{\ell,k,n} = 1$) or not on interval n.

We represent the problem of finding the maximal flow between capacity-constrained queues as a Linear Program (LP) over the following variables defined for all interval $n \in \{1, \ldots, \mathrm{N}\}$ and queues i and j:

- $q_{i,n} \in [0, \mathrm{Q}_i]$, traffic volume waiting in the stop line of queue i at the beginning of interval n;
- $f_{i,n}^{\mathrm{in}} \in [0, I_{i,n}]$, inflow to the network via queue i during interval n;
- $f_{i,n}^{\mathrm{out}} \in [0, \mathrm{F}_i^{\mathrm{out}}]$, outflow from the network via queue i during interval n; and
- $f_{i,j,n} \in [0, \mathrm{F}_{i,j}]$, flow from queue i into queue j during interval n.

The maximum traffic flow from queue i to queue j is enforced by constraints (C1) and (C2). (C1) ensures that only the fraction $\mathrm{Pr}_{i,j}$ of the total internal outflow of i goes to j, and (C2) forces the flow from i to j to be zero if all phases

controlling i are inactive. (i.e., $p_{\ell,k,n} = 0$ for all $k \in \mathcal{Q}_i^{\mathcal{P}}$).

$$f_{i,j,n} \leq \mathrm{Pr}_{i,j} \sum_{k=1}^{|\mathcal{Q}|} f_{i,k,n} \tag{C1}$$

$$f_{i,j,n} \leq \mathrm{F}_{i,j} \sum_{p_{\ell,k,n} \in \mathcal{Q}_i^{\mathcal{P}}} p_{\ell,k,n} \tag{C2}$$

To simplify the presentation of the remainder of the LP, we define the helper variables $q_{i,n}^{\mathrm{in}}$ (C3) and $q_{i,n}^{\mathrm{out}}$ (C4) to, respectively, represent the volume of traffic to enter and leave queue i during interval n, and $t_n = \sum_{x=1}^{n} \Delta t_x$ to represent the time elapsed since the beginning of the problem until the end of interval Δt_n.

$$q_{i,n}^{\mathrm{in}} = \Delta t_n (f_{i,n}^{\mathrm{in}} + \sum_{j=1}^{|\mathcal{Q}|} f_{j,i,n}) \tag{C3}$$

$$q_{i,n}^{\mathrm{out}} = \Delta t_n (f_{i,n}^{\mathrm{out}} + \sum_{j=1}^{|\mathcal{Q}|} f_{i,j,n}) \tag{C4}$$

In order to account for the case where $\mathrm{T}_i^{\mathrm{p}}$ is larger than Δt, we need to find the volume of traffic that entered queue i between two points in time x and y. This volume of traffic, denoted as $V_i(x, y)$, is obtained by integrating $q_{i,n}^{\mathrm{in}}$ over $[x, y]$ and is defined in (1) where $T^{-1}(x)$ is the function that returns $j \in \{0, \ldots, N\}$ such that x equals t_j (i.e., the j-th time step). Since we assumed that $\mathrm{T}_i^{\mathrm{p}}$ is divisible by the different $\mathrm{T}_i^{\mathrm{p}}$, $T^{-1}(x)$ is always well-defined, i.e., there always exists j such that x equals t_j. Because the QTM dynamics are *piecewise linear*, $q_{i,n}^{\mathrm{in}}$ is a step function w.r.t. time and this integral reduces to the sum of $q_{i,n}^{\mathrm{in}}$ over the intervals between $T^{-1}(x)$ and $T^{-1}(y)$.

$$V_i(x, y) = \sum_{k=T^{-1}(x)}^{T^{-1}(y)} q_{i,k}^{\mathrm{in}} \tag{1}$$

Using these helper variables, (C5) represents the flow conservation principle for queue i where $V_i(t_{n-1} - \mathrm{T}_i^{\mathrm{p}}, t_n - \mathrm{T}_i^{\mathrm{p}})$ is the volume of cars that reached the stop line during Δt_n. Notice that (C5) represents a non-first order Markovian update because the update considers the previous $n - T^{-1}(t_n - \mathrm{T}_i^{\mathrm{p}})$ time steps, i.e., the number of Δt_n spanned in $\mathrm{T}_i^{\mathrm{p}}$. To ensure that the total volume of traffic traversing i (i.e., $V_i(t_n - \mathrm{T}_i^{\mathrm{p}}, t_n)$) and waiting at the stop line does not exceed the capacity of the queue, we apply (C6).

$$q_{i,n} = q_{i,n-1} - q_{i,n-1}^{\mathrm{out}} + V_i(t_{n-1} - \mathrm{T}_i^{\mathrm{p}}, t_n - \mathrm{T}_i^{\mathrm{p}}) \tag{C5}$$

$$V_i(t_n - \mathrm{T}_i^{\mathrm{p}}, t_n) + q_{i,n} \leq \mathrm{Q}_i \tag{C6}$$

As with MILP formulations of CTM (e.g., Lin and Wang (2004)), QTM is also susceptible to *withholding traffic*, i.e., the optimizer might prevent cars from moving from i to j even though the associated traffic phase is active and j is not full. This might be used by the optimizer to reserve space for traffic from an alternate queue to further minimize delay in the long-term, even though it leads to unintuitive traffic flow behavior. We address this well-known issue through our objective function (O1) by maximizing the external outflow $f_{i,n}^{\mathrm{out}}$ and external inflow $f_{i,n}^{\mathrm{in}}$ of all queues i. This quantity is weighted by the remaining time until the end of the problem horizon T to force the optimizer to allow as much traffic volume as possible into the network and move traffic to the outside of the network as soon as possible.

$$\max \sum_{n=1}^{\mathrm{N}} \sum_{i=1}^{|\mathcal{Q}|} (\mathrm{T} - t_n + 1)(f_{i,n}^{\mathrm{out}} + f_{i,n}^{\mathrm{in}}) \tag{O1}$$

The objective (O1) corresponds to minimizing delay in CTM models, e.g., (O1) is equivalent to the objective function (O3) in Lin and Wang (2004) for their parameters parameters $\alpha = 1$, $\beta = 1$ for the origin cells, and $\beta = 0$ for all other cells.

3 Traffic Control with MILP-encoded QTM

In this section, we show how to compute the optimized adaptive control plan by extending the LP (O1, C1–C6) into an Mixed-Integer LP (MILP). Formally, for all $\ell \in \mathcal{L}$, $k \in \mathcal{P}_\ell$, and interval $n \in \{1, \ldots, N\}$, the phase activation parameter $p_{\ell,k,n} \in \{0, 1\}$ becomes a free variable to be optimized. In order to obtain a valid control plan, we enforce that one phase of traffic light ℓ is always active at any interval n (C7) and cyclic phase policies where phase changes follow a fixed ordered sequence, indexed by k (C8) (where (C8) assumes that $k + 1$ equals 1 if $k = |\mathcal{P}_\ell|$).

$$\sum_{k=1}^{|\mathcal{P}_\ell|} p_{\ell,k,n} = 1 \tag{C7}$$

$$p_{\ell,k,n-1} \leq p_{\ell,k,n} + p_{\ell,k+1,n} \tag{C8}$$

Next, we enforce the minimum and maximum phase durations (i.e., $\Phi_{\ell,k}^{\min}$ and $\Phi_{\ell,k}^{\max}$) for each phase $k \in \mathcal{P}_\ell$ of traffic light ℓ. To encode these constraints, we use the helper variable $d_{\ell,k,n} \in [0, \Phi_{\ell,k}^{\max}]$, defined by constraints (C9–C13), that: (i) holds the elapsed time since the start of phase k when $p_{\ell,k,n}$ is active (C9,C10); (ii) is constant and holds the duration of the last phase until the next activation when $p_{\ell,k,n}$ is inactive (C11,C12); and (iii) is restarted when phase k changes from inactive to active (C13). Notice that (C9–C13) employs the *big-M* method to turn the cases that should not be active into subsumed constraints based on the value of $p_{\ell,k,n}$. We use $\Phi_{\ell,k}^{\max}$ as our large constant since $d_{\ell,k,n} \leq \Phi_{\ell,k}^{\max}$ and $\Delta t_n \leq \Phi_{\ell,k}^{\max}$. Similarly, constraint (C14) ensures the minimum phase time of k and is not enforced while k is still active.

$$d_{\ell,k,n} \leq d_{\ell,k,n-1} + \Delta t_{n-1} p_{\ell,k,n-1} + \Phi_{\ell,k}^{\max}(1 - p_{\ell,k,n-1}) \tag{C9}$$

$$d_{\ell,k,n} \geq d_{\ell,k,n-1} + \Delta t_{n-1} p_{\ell,k,n-1} - \Phi_{\ell,k}^{\max}(1 - p_{\ell,k,n-1}) \tag{C10}$$

$$d_{\ell,k,n} \leq d_{\ell,k,n-1} + \Phi_{\ell,k}^{\max} p_{\ell,k,n-1} \tag{C11}$$

$$d_{\ell,k,n} \geq d_{\ell,k,n-1} - \Phi_{\ell,k}^{\max} p_{\ell,k,n} \tag{C12}$$

$$d_{\ell,k,n} \leq \Phi_{\ell,k}^{\max}(1 - p_{\ell,k,n} + p_{\ell,k,n-1}) \tag{C13}$$

$$d_{\ell,k,n} \geq \Phi_{\ell,k}^{\min}(1 - p_{\ell,k,n}) \tag{C14}$$

Lastly, we constrain the sum of all the phase durations for light ℓ to be within the cycle time limits $\Psi_\ell^{\min}$ (C15) and $\Psi_\ell^{\max}$ (C16). In both (C15) and (C16), we use the duration of phase 1 of ℓ from the previous interval $n-1$ instead of the current interval n because (C13) forces $d_{\ell,1,n}$ to be 0 at the beginning of each cycle; however, from the previous end of phase 1 until $n-1$, $d_{\ell,1,n-1}$ holds the correct elapse time of phase 1. Additionally, (C15) is enforced right after the end of the each cycle, i.e., when its first phase is changed from inactive to active.

$$d_{\ell,1,n-1} + \sum_{k=2}^{|\mathcal{P}_\ell|} d_{\ell,k,n} \geq \Psi_\ell^{\min}(p_{k,1,n} - p_{k,1,n-1}) \quad \text{(C15)}$$

$$d_{\ell,1,n-1} + \sum_{k=2}^{|\mathcal{P}_\ell|} d_{\ell,k,n} \leq \Psi_\ell^{\max} \quad \text{(C16)}$$

The MILP (O1, C1–C16) encodes the problem of finding the optimized adaptive traffic control plan in a QTM network without light rail.

Light Rail Constraints To incorporate a fixed-schedule light rail in our model, we post-process our MILP model by fixing the free variable $p_{\ell,k,n}$ for all n such that the light rail uses phase k of ℓ at time n. Formally, given a schedule $S_\ell(k,n) \in \{0,1\}$ where 1 represents that the light rail uses phase k of ℓ at time n, we replace (C9–C14) by (C17) and (C18) when $\sum_{k\in\mathcal{P}_\ell} S_\ell(k,n) > 0$.

$$p_{\ell,k,n} = S_\ell(k,n) \quad \text{(C17)}$$

$$d_{\ell,k,n} = d_{\ell,k,n-1} \quad \text{(C18)}$$

(C17) enforces that the correct phase k is active when the light rail reaches the traffic light l, and (C18) ensures that the light rail can pass through l even if more than the maximum phase time $\Phi_{\ell,k}^{\max}$ is necessary.

3.1 QTM as a Fixed-Time Controller

We can further extend QTM to compute an optimized control plan with fixed phase durations. For all $\ell \in \mathcal{L}$, $k \in \mathcal{P}_\ell$, we introduce the new variable $\phi_{\ell,k}^{\text{fixed}} \in [\Phi_{\ell,k}^{\min}, \Phi_{\ell,k}^{\max}]$ and replace the bounds constraints on $d_{\ell,k,n}$ (that is, $d_{\ell,k,n} \leq \Phi_{\ell,k}^{\max}$ and C14) with fixed the duration constraints (C19-C20).

$$d_{\ell,k,n} \leq \phi_{\ell,k}^{\text{fixed}} + \Phi_{\ell,k}^{\max} p_{\ell,k,n} \quad \text{(C19)}$$

$$d_{\ell,k,n} \geq \phi_{\ell,k}^{\text{fixed}} - \Phi_{\ell,k}^{\max} p_{\ell,k,n} \quad \text{(C20)}$$

Similarly to the variable phase duration constraints, the *big-M* method is employed to enforce (C19-C20) only while the phase is inactive. Furthermore, these constraints are only applied over time intervals n such that $t_n > \Psi_\ell^{\max}$ in order to allow the controller to optimize an initial phase offset at the start of the plan.

4 Empirical Evaluation

In this section we compare the solutions for traffic networks modeled as a QTM before and after the introduction of a light rail. We consider both fixed-time control, i.e., a non-adaptive control plan, and optimized adaptive control obtained by solving the MILP (O1, C1–C18). The obtained solutions are simulated using a microsimulator and their total travel time and observed delay distribution are used as comparison metrics. Our hypothesis is that the optimized adaptive approach is able to mitigate the impact of introducing light rail w.r.t. both metrics. In the remainder of this section, we present the traffic networks considered in the experiments, our methodology, and the results.

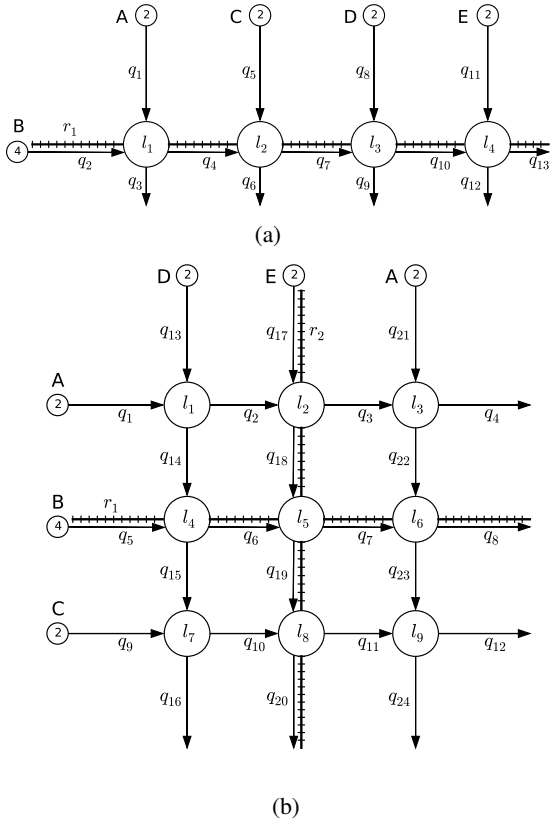

Figure 2: Networks used to evaluate the performance: (a) an arterial road with parallel light rail; (b) an urban grid with crisscrossing streets and light rail.

4.1 Networks

We consider two networks of differing complexity: an arterial crossed by four side streets (Figure 2a) and a 3-by-3 grid (Section 4.1). The queues receiving cars from outside of the network are marked in Figure 2 and we refer to them as input queues. The maximum queue capacity (Q_i) is 60 vehicles for non-input queues and infinity for input queues to prevent interruption of the input demand due to spill back from the stop line. The free flow speed is 50 km/h and the traversal time of each queue i ($\mathrm{T}_i^{\mathrm{p}}$) is set at 30s, except for the output queues on Network 1 where the traversal time is 10s. For each street, flows are defined from the head of each queue i into the tail of the next queue j; there is no turning traffic ($\mathrm{Pr}_{i,j} = 1$), and the maximum flow rate between

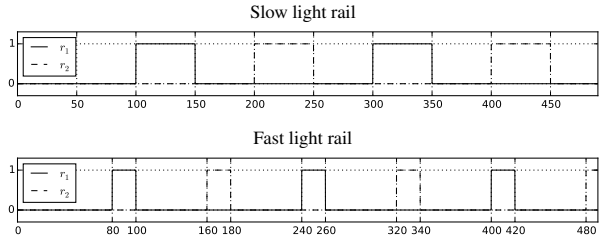

Figure 3: Light rail schedule functions.

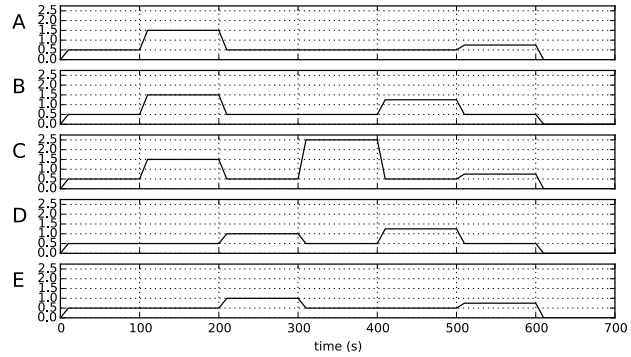

Figure 4: Weight functions for generating demand profiles.

queues, $\mathrm{F}_{i,j}$, is set at 0.5 vehicles/s. All traffic lights have two phases, north-south and east-west, and for each traffic light ℓ and phase k, $\Phi^{\min}_{\ell,k}$ is 10s, $\Phi^{\max}_{\ell,k}$ is 30s, $\Psi^{\min}_{\ell}$ is 20s, and $\Psi^{\max}_{\ell}$ is 60s.

4.2 Experimental Methodology

We evaluate each network using both fixed-time control and the optimized adaptive control in two scenarios: before the introduction of light rail and after. For the latter scenario, we consider the two different light rail schedules depicted in Figure 3: a slow light rail with a crossing duration of 50s, a period of 200s, and a travel time of 100s between lights; and a fast light rail with a crossing duration of 20s, period of 160s, and travel time of 80s between lights. On Network 2, the North-South schedule is offset by 100s for the slow light rail and 80s for the fast light rail to avoid a collision at l_5.

Each network is evaluated at increasing demand levels up to the point where $f^{\text{in}}_{i,n}$ becomes saturated. For each demand level, traffic is injected into the network in bursts for 600s, and the number of cars entering the network through i at time n is defined as $I_{i,n} = \max(\alpha\beta \mathrm{w}_i(t_n), \beta)$ where: w_i is the weight function in Figure 4 corresponding to the letter label of i in Figure 2; β is the maximum inflow rate in vehicles per Δt_n, as annotated at the start of queue i in Figure 2; and $\alpha \in (0, 2]$ is the scaling factor for the demand level being evaluated.

For each evaluation, we first generate a signal plan using QTM configured as either an optimized adaptive controller or a fixed-time controller. We use a problem horizon T large enough, typically in the range 1000s – 1500s, to allow all traffic to clear the network, that lets us measure the incurred delay in all the cars. Next, we microsimulate the signal plans on their respective the networks using the Intelligent Driver Model (IDM) (Treiber, Hennecke, and Helbing 2000). For the microsimulation, all vehicles have identical IDM parameters: length $l = 3$ m, desired velocity $v_0 = 50$ km/h, safe time headway $T = 1.5$ s, maximum acceleration $a = 2$ m/s^2, desired deceleration $b = 3$ m/s^2, acceleration exponent $\delta = 4$, and jam distance $s_0 = 2$ m. We follow the same demand profiles used for computing the signal plans for the microsimulation.

For all experiments, we used Gurobi as the MILP solver running on a heterogeneous cluster with 2.8GHz AMD Opteron 4184, 3.1GHz AMD Opteron 4334 (12 cores each), and 2Ghz Intel Xeon E5405 (4 cores). We use 4 cores for each run of the solver. We limit the MIP gap accuracy to 0.02% and 0.1% for the arterial and grid networks, respectively. Due to Gurobi's stochastic strategies, runtimes for the solver can vary, and we do not set a time limit. The optimized adaptive solution are typically found in real time (less than 200s), while fixed-time plans can take significantly longer (on average 4000s for a 1000s horizon); however, once the fixed-time solution is found, it can be deployed indefinitely.

4.3 Results

Figures 5a and 5b show, for each network, the average delay per vehicle as a function of demand for both optimized fixed-time and optimized adaptive control approaches in three scenarios: before the light rail and after the installation of light rail using the slow and the fast schedules. As we hypothesized, optimized adaptive control is able to mitigate the impact of the introduction of light rail and it marginally increases the average delay when compared with the average delay produced by fixed-time controller **before** the light rail. Moreover, as shown in Figures 5c and 5d, the optimized adaptive controller also produces better signal plans than the fixed-time controller, i.e., plans with smaller median, third quartile, and maximum delay. Over all our experiments, the maximum observed delay for the optimized adaptive signal plans after the introduction of light rail is no more than the double of the maximum delay before the light rail. Figure 7 provides more details on the behavior of the signal plans for demand level II (Figures 5a and 5b) by showing the cumulative number of cars by number of observed stops. Note that in Figures 7a and 7b the fixed-time controller chooses to prioritize the arterial over the side streets, but overall (Figure 7c) the optimized controller does better with less stops at all frequencies.

To further illustrate the benefits of using optimized adaptive control to minimize the impact of adding light rail to traffic network, Figure 6 shows the impact on average delay as a function of the percentage of cars that are switching to the light rail. In these plots, the demand level is fixed and higher values are better (i.e., there is a decrease in the average delay) and zero means that there is no change after installing light rail. For the three combinations of before and after policies presented, we can see that, while keeping the fixed-time controller requires from 7.5% to 40% of the drives to switch to light rail in order to obtain the same av-

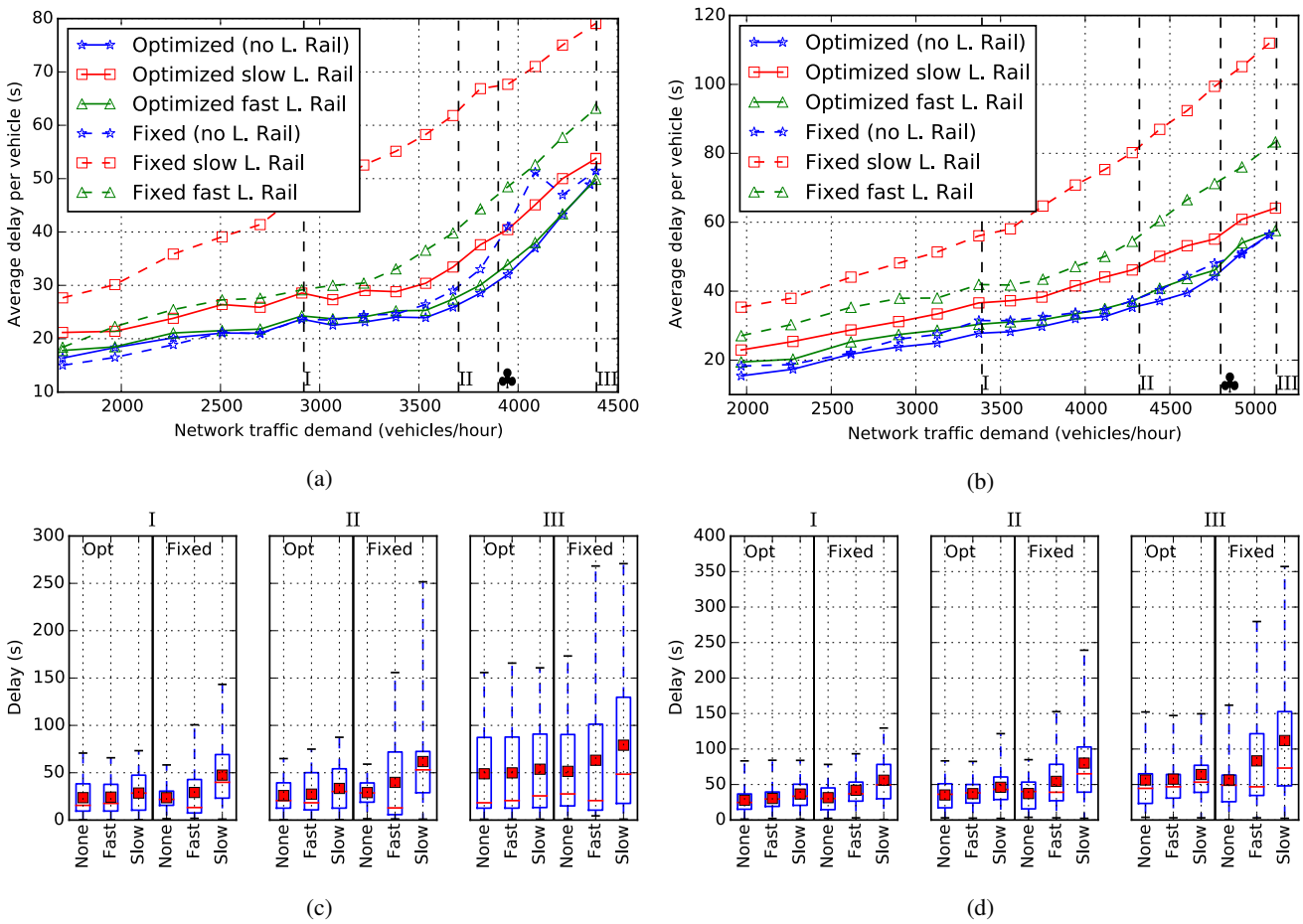

Figure 5: Average delay by the network demand for the arterial (a) and grid (b) networks. Box plots representing the observed distribution of delay for 3 different values of demand for each network (c,d). The mean is presented as a red square in the box plots.

erage delay as before its installation, the optimized adaptive approach requires only from 2.5% to 10% of the drivers to switch when already using optimized adaptive control **before** the light rail. When compared fixed-time before the light rail and optimized adaptive after, the average delay stays the same if only the 2% and 5% of the drives switch to the light rail when considering the slow light rail schedule in the arterial and grid networks, respectively; moreover, the average delay **decreases** for both networks using the fast light rail schedule even if no driver switches to the newly installed public transportation.

Figure 8 shows microsimulation time-distance plots for several streets in Network 1. The y-axis of the plot shows the distance along the street, and the x-axis shows the evolution over time. Each colored trace represents the journey of a vehicle along the street. Traffic signals at fixed distances down the street appear as black horizontal dashed lines, where a solid bar represents that the phase is inactive, that the light is red, and traffic cannot pass. Where the line is broken the phase is active, the light is green and cars can proceed past. The time-distance plots capture the queueing behaviour of the traffic as each vehicle decelerates when approaching congested traffic, or red or amber light ahead. When the trace of a vehicle is horizontal, it has become stationary. From the microsimulation time-distance plots of the side streets (Figure 8) we can see that the fixed-adaptive controller has prioritized the arterial phase duration over the side street duration, to achieve coordinated "green corridors", sized for the average traffic density in the network, and suffers from accumulative queue build up in the side streets following each transit of the light rail. Conversely, the optimized controller is able to clear out the queue build up in the side streets by increasing the phase time of the side street for a cycle after the transit has passed through, and then returns to a schedule that prioritises the arterial depending on the changes in traffic density. When the traffic density in the arterial is higher than the side streets then the optmized controller will coordinate "green corridors" along the arterial.[1]

[1]The supplementary material further elucidates this point.

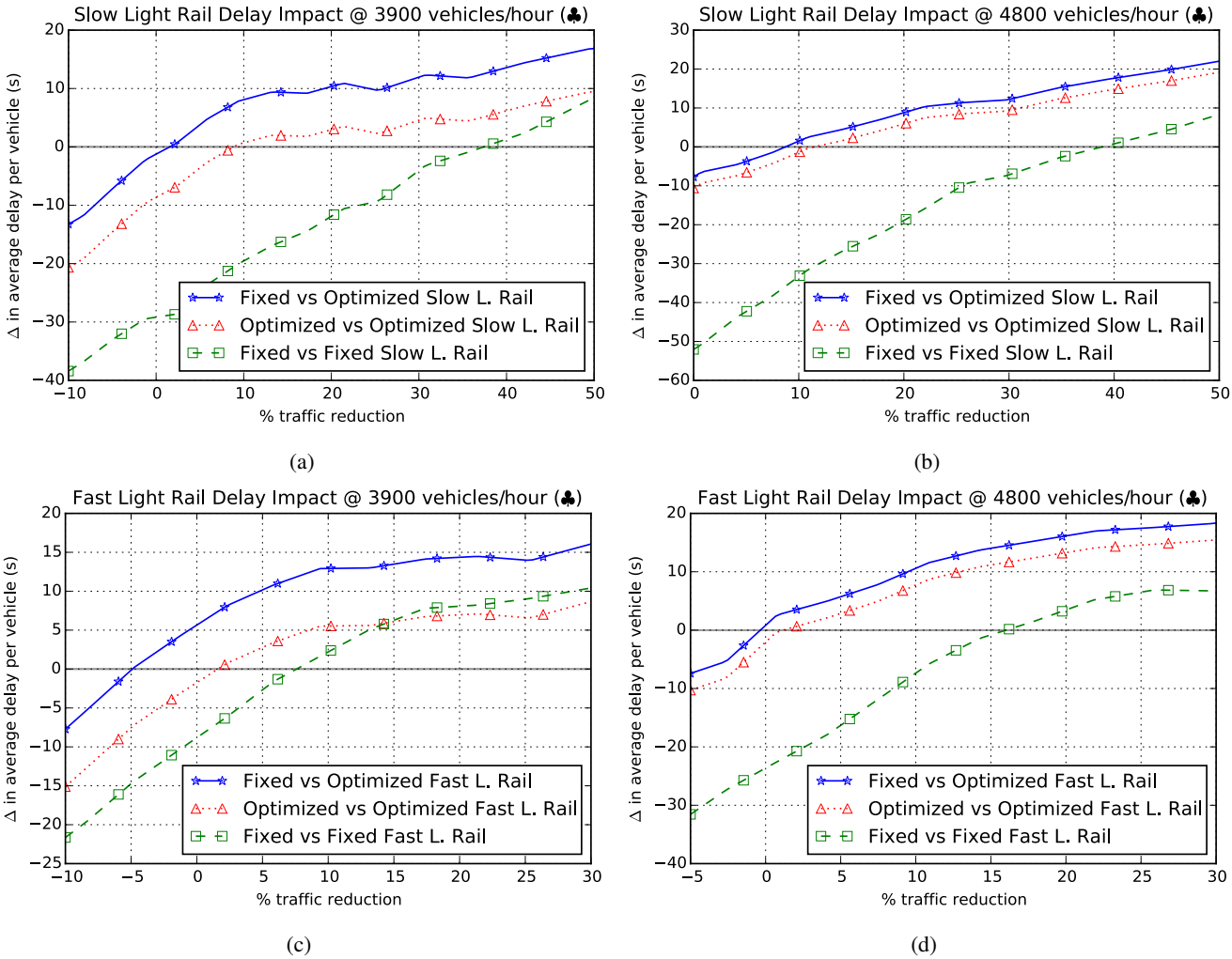

Figure 6: Impact on average delay for the arterial (first column) and grid (second column) networks for both light rail schedules (rows) in different scenarios (curves) of traffic control system before and after installation of light rail. The x-axis is the percentage of cars switching to the public transportation and the y-axis is the impact after the light rail is installed. Negative impact represents increase in average delay. The vehicle demand for (a-d) are marked as ♣ in their respective plots in Figure 5.

5 Conclusion

In this paper, we show how our optimized adaptive traffic signal control method based on Mixed Integer Linear Programming (MILP) can be used for mitigating the impact of installing light rail on conventional traffic networks. Our experiments with the QTM model of traffic flow show that our method is able to minimize the impact on the average delay with respect to fixed-time signal control and also finds better quality solutions, i.e., solutions with substantially lower third quartile and maximum observed delay. These improvements were also verified in a non-QTM based microsimulation model to validate performance improvements w.r.t. a finer-grained nonlinear model of traffic flow (e.g., with acceleration and queue-length effects). Ultimately our results demonstrate a way to optimize conventional fixed time controllers w.r.t. light rail schedule constraints; furthermore, when these methods are extended to our fully optimized adaptive controller, it leads to a win-win situation where both conventional vehicle traffic and light rail commuters benefit through the application of MILP-based optimization *regardless* of the reduction in conventional traffic that opts to take light rail.

For future work, a key question to resolve is how large we can scale the traffic and light rail network before we need to investigate decomposition-based approaches to scaling the solution (e.g, MILP-based methods like dual decomposition or region-based traffic network partitioning schemes). Future work should also examine the (online) learnability of the QTM model from different traffic sensor data ranging from conventional inductive (double) loop counters through to video feeds. Finally, noting that the nonlinear microsimulation model offers a higher-fidelity model of actual traffic behavior, future work should consider expanding the QTM to model nonlinear traffic flows (Lu, Dai, and Liu 2011;

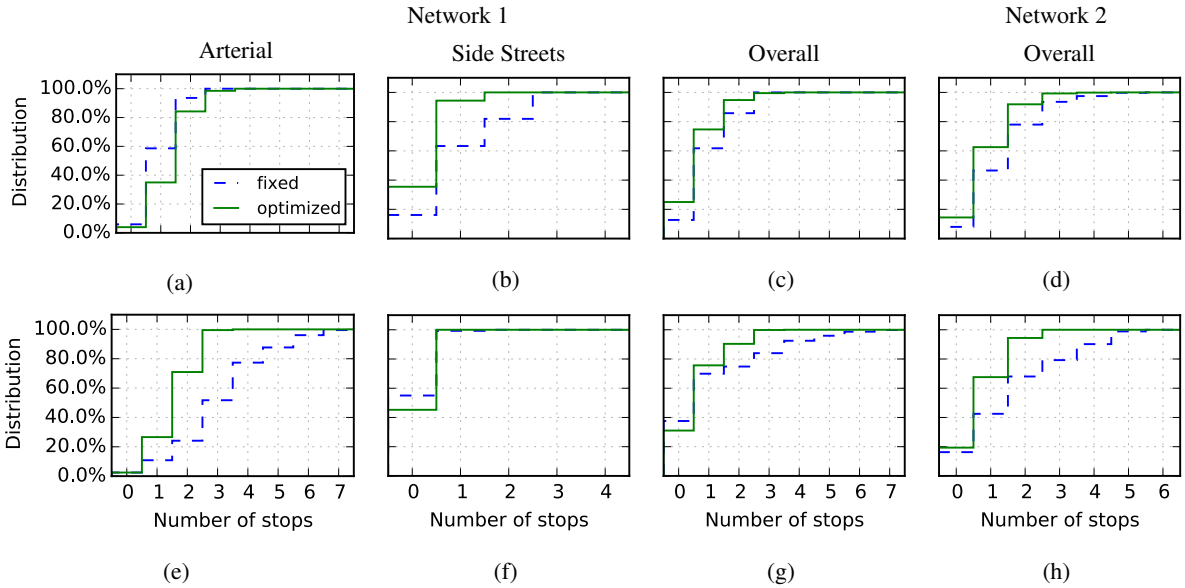

Figure 7: Impact of controller on number of stops. Top row is for the slow light rail schedule. Bottom row is for the fast light rail schedule

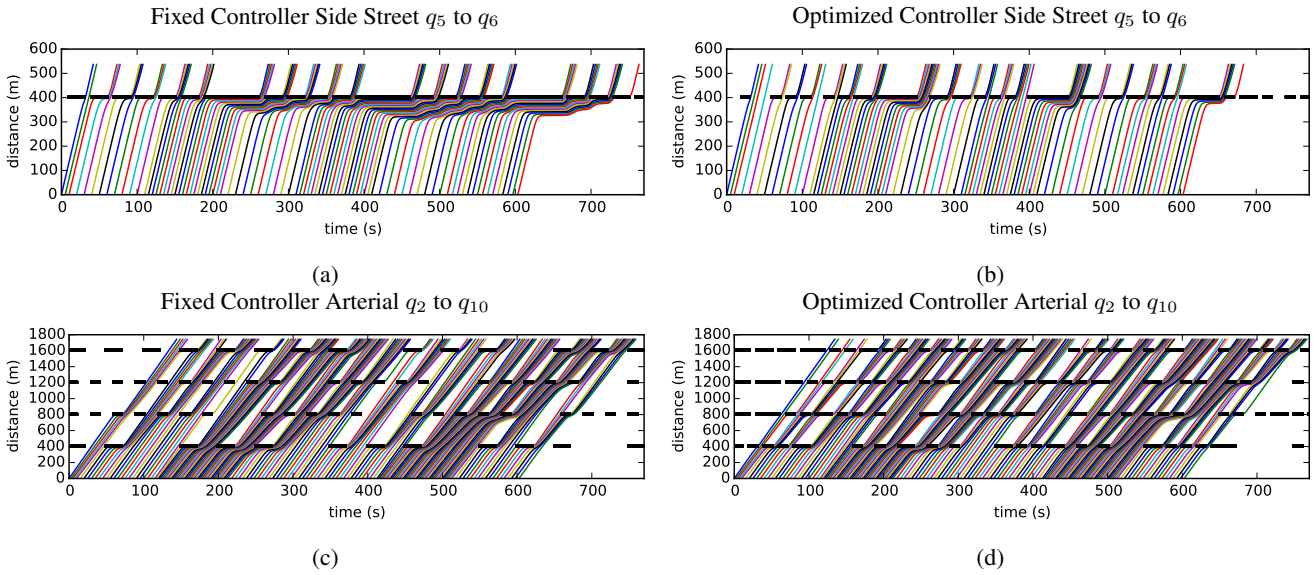

Figure 8: Microsimulation time-distance plots of side street q_5 to q_6 and arterial q_2 to q_{13} in Network 1 with the slow light rail schedule. The fixed-adaptive controller has prioritized the arterial phase duration (c) over the side street duration (a) and suffers from accumulative queue build up in the side streets following each transit of the light rail. The optimized controller is able to clear out the queue build up in the side streets by increasing the phase time of the side street (b) for a cycle after the transit has passed through, and then returns to a schedule that prioritizes the arterial (d) depending on the changes in traffic density.

Muralidharan, Dervisoglu, and Horowitz 2009; Kim 2002; Huang 2011) and investigating the benefits of nonlinear optimization in this setting relative to the existing QTM.

Notwithstanding this important future work, our key results demonstrate for the first time the potential of MILP-based traffic signal control approaches to nullify the impact of installing light rail on conventional traffic. Consequently, the use of such optimized controllers as proposed here could remove this critical public concern of light rail installation and thus positively impact the environment, urban productivity, and commute time reductions for both conventional traffic and public transit riders as a result.

References

[Anonymous 2016] Anonymous. 2016. A non-homogenous time mixed integer LP formulation for traffic signal control.

In *Transport Research Board (TRB) Annual Meeting*.

[Bazzan and Klügl 2013] Bazzan, A. L. C., and Klügl, F. 2013. *Introduction to Intelligent Systems in Traffic and Transportation*. Synthesis Lectures on Artificial Intelligence and Machine Learning. Morgan & Claypool Publishers.

[El-Tantawy, Abdulhai, and Abdelgawad 2013] El-Tantawy, S.; Abdulhai, B.; and Abdelgawad, H. 2013. Multiagent reinforcement learning for integrated network of adaptive traffic signal controllers (marlin-atsc): methodology and large-scale application on downtown Toronto. *Intelligent Transportation Systems, IEEE Transactions on* 14(3):1140–1150.

[Gartner and Stamatiadis 2002] Gartner, N. H., and Stamatiadis, C. 2002. Arterial-based control of traffic flow in urban grid networks. *Mathematical and computer modelling* 35(5):657–671.

[Han, Friesz, and Yao 2012] Han, K.; Friesz, T. L.; and Yao, T. 2012. A link-based mixed integer lp approach for adaptive traffic signal control. *arXiv preprint arXiv:1211.4625*.

[He et al. 2010] He, Q.; Lin, W.-H.; Liu, H.; and Head, K. L. 2010. Heuristic algorithms to solve 0–1 mixed integer lp formulations for traffic signal control problems. In *Service Operations and Logistics and Informatics (SOLI), 2010 IEEE International Conference on*, 118–124. IEEE.

[He, Head, and Ding 2011] He, Q.; Head, K. L.; and Ding, J. 2011. Pamscod: Platoon-based arterial multi-modal signal control with online data. *Procedia-Social and Behavioral Sciences* 17:462–489.

[Huang 2011] Huang, K. C. 2011. *Traffic Simulation Model for Urban Networks: CTM-URBAN*. Ph.D. Dissertation, Concordia University.

[Hunt et al. 1981] Hunt, P. B.; Robertson, D. I.; Bretherton, R. D.; and Winton, R. I. 1981. Scoot–a traffic responsive method of coordinating signals. Technical report, Transportation Road Research Lab, Crowthorne, U.K.

[Kim 2002] Kim, Y. 2002. Online traffic flow model applying dynamic flow-density relation. Technical report, Int. At. Energy Agency.

[Li and Zhang 2014] Li, J., and Zhang, H. 2014. Coupled linear programming approach for decentralized control of urban traffic. *Transportation Research Record: Journal of the Transportation Research Board* (2439):83–93.

[Lin and Wang 2004] Lin, W.-H., and Wang, C. 2004. An enhanced 0-1 mixed-integer lp formulation for traffic signal control. *Intelligent Transportation Systems, IEEE Transactions on* 5(4):238–245.

[Lo, Chang, and Chan 1999] Lo, H. K.; Chang, E.; and Chan, Y. C. 1999. Dynamic network traffic control. *Transportation Research Part A: Policy and Practice* 35(8):721–744.

[Lo 1998] Lo, H. K. 1998. A novel traffic signal control formulation. *Transportation Research Part A: Policy and Practice* 33(6):433–448.

[Lu, Dai, and Liu 2011] Lu, S.; Dai, S.; and Liu, X. 2011. A discrete traffic kinetic model–integrating the lagged cell transmission and continuous traffic kinetic models. *Transportation Research Part C: Emerging Technologies* 19(2):196–205.

[Muralidharan, Dervisoglu, and Horowitz 2009] Muralidharan, A.; Dervisoglu, G.; and Horowitz, R. 2009. Freeway traffic flow simulation using the link node cell transmission model. In *American Control Conference, 2009. ACC'09.*, 2916–2921. IEEE.

[Sims and Dobinson 1980] Sims, A. G., and Dobinson, K. W. 1980. Scat–the sydney co-ordinated adaptive traffic system: Philosophy and benefits. *IEEE Transactions on Vehicular Technology* 29.

[Smith et al. 2013] Smith, S.; Barlow, G.; Xie, X.-F.; and Rubinstein, Z. 2013. Surtrac: Scalable urban traffic control. In *Transportation Research Board 92nd Annual Meeting Compendium of Papers*. Transportation Research Board.

[Thompson 2003] Thompson, G. L. 2003. Defining an alternative future: Birth of the light rail movement in north america. In *Transportation Research Board (TRB) Annual Meeting*.

[Treiber, Hennecke, and Helbing 2000] Treiber, M.; Hennecke, A.; and Helbing, D. 2000. Congested traffic states in empirical observations and microscopic simulations. *Physical Review E* 62(2):1805.

[Varaiya 2013] Varaiya, P. 2013. Max pressure control of a network of signalized intersections. *Transportation Research Part C: Emerging Technologies* 36:177–195.

[Xie, Smith, and Barlow 2012] Xie, X.-F.; Smith, S. F.; and Barlow, G. J. 2012. Schedule-driven coordination for real-time traffic network control. In *ICAPS*.